Performance of mmWave-Based Mesh Networks in Indoor Environments with Dynamic Blockage

Rustam Pirmagomedov[1,2(✉)], Dmitri Moltchanov[2], Viktor Ustinov[3], Md Nazmus Saqib[2], and Sergey Andreev[2]

[1] Peoples' Friendship University of Russia (RUDN University), 6 Miklukho-Maklaya St, Moscow 117198, Russian Federation
prya.spb@gmail.com
[2] Tampere University, Korkeakoulunkatu 1, 33720 Tampere, Finland
[3] St. Petersburg State University of Telecommunication, Bolshevikov 22/1, St. Petersburg 190000, Russian Federation

Abstract. Due to growing throughput demands dictated by innovative media applications (e.g., 360° video streaming, augmented and virtual reality), millimeter-wave (mmWave) wireless access is considered to be a promising technology enabler for the emerging mobile networks. One of the crucial usages for such systems is indoor public protection and disaster relief (PPDR) missions, which may greatly benefit from higher mmWave bandwidths. In this paper, we assess the performance of on-demand mmWave mesh topologies in indoor environments. The evaluation was conducted by utilizing our system-level simulation framework based on a realistic floor layout under dynamic blockage conditions, 3GPP propagation model, mobile nodes, and multi-connectivity operation. Our numerical results revealed that the use of multi-connectivity capabilities in indoor deployments allows for generally improved connectivity performance whereas the associated per-node throughput growth is marginal. The latter is due to the blockage-rich environment, which is typical for indoor layouts as it distinguishes these from outdoor cases. Furthermore, the number of simultaneously supported links at each node that is required to enhance the system performance is greater than two, thus imposing considerable control overheads.

Keywords: Milliliter-wave mesh · 5G NR · PPDR · Emergency response · Indoor environment

1 Introduction

Due to the growing capacity requirements on the air interface as demanded by innovative media applications, such as 360° HD streaming, augmented and virtual reality (AR/VR), millimeter-wave (mmWave) wireless access is considered as a promising technology for future mobile networks.

The publication has been prepared with the support of the "RUDN University Program 5-100". This work was also supported by the project TAKE-5: The 5th Evolution Take of Wireless Communication Networks, funded by Business Finland.

Published by Springer Nature Switzerland AG 2019
M. Di Felice et al. (Eds.): WWIC 2019, LNCS 11618, pp. 129–140, 2019.
https://doi.org/10.1007/978-3-030-30523-9_11

In addition to their undisputed benefits, mmWave networks bring new challenges to systems designers, which include high propagation losses, sensitivity to blockage by obstacles, and beamsteering functionality for highly directive transmission [1]. Particularly, free space propagation loss at 60 GHz is 28 decibels higher than that at 2.4 GHz [2]. For these reasons, mmWave links are highly directional, and they use steerable antenna arrays with sufficient gain to compensate for these extreme losses. Moreover, due to shorter wavelength (approximately 5 mm at 60 GHz), even small objects may block the mmWave link [3]. Finally, mmWave connections are highly affected by atmospheric and molecular absorption [4]. Altogether these three factors significantly affect the reliability of mmWave communication.

In addition to conventional setups, such as cellular systems where 3GPP is currently at the completion phase of the New Radio (NR) standardization, the extreme throughputs make mmWave communications technology appealing for extending the conventional mobile access by implementing wireless mesh networking. The mmWave mesh topologies may improve coverage of mmWave access points by utilizing multi-hop links and at the same time enhance communications reliability with multi-connectivity operation [5]. One of the crucial use cases in this context is public protection and disaster relief (PPDR) missions, which may greatly benefit from using 360° HD streaming and AR/VR applications enabled by bandwidth-rich mmWave communications technology.

Performance of mmWave systems with multi-connectivity capabilities in outdoor environments has been investigated thoroughly. An upper bound for the capacity of multi-connectivity mmWave systems has been obtained in [6]. This bound has been refined in [7,8]. Recently, engineering studies addressing multi-connectivity aspects of mmWave networks have started to emerge [9,10]. These works reveal that multi-connectivity operation improves both outage probability and system throughput non-incrementally. These results have been extended to mmWave mesh deployments in the outdoor use cases in [11–13], where the multi-connectivity operation has also been shown to considerably improve the network connectivity and throughput.

Compared to outdoor environments, indoor mmWave mesh deployments bring additional challenges that are primarily caused by an extremely complex propagation process. The use of mmWave meshes in dynamic PPDR use cases, such as fire suppression missions where the environment may change dynamically, adds another level of complexity. Notably, link blockage in such indoor scenarios is induced by the interior of buildings (e.g., partitions, walls) as well as mobile objects (e.g., people, moving equipment). Taking into account the potential mobility of nodes, indoor mmWave mesh deployments are expected to be highly dynamic, with continuously changing connectivity patterns between the mesh nodes. In these conditions, multi-connectivity can be considered as an efficient enabler for both maintaining network connectivity and improving its throughput.

In this paper, we evaluate the performance of mmWave mesh systems in a realistic indoor environment characterized by the mobility of nodes, dynamic blockers, 3GPP-compatible propagation model, and multi-connectivity operation.

Fig. 1. Nodes on the layout during simulation 2D view.

Particularly, we consider our PPDR scenario as an illustrative use case for investigating network connectivity and throughput characteristics. Our main findings are:

- the use of multi-connectivity operation drastically improves mmWave mesh connectivity in indoor deployments but its effect on the per-node throughput is minor;
- to augment connectivity and throughput in dense indoor mmWave mesh topologies, the number of simultaneously supported links needs to be greater than two, thus implying considerable control signaling overheads.

The rest of this text is organized as follows. In Sect. 2, we introduce the system model and its components. Our system-level simulation framework and data collection/analysis procedures are described in Sect. 3. We report our results in Sect. 4. Conclusions are provided in the last section.

2 System Model

In this section, we introduce our system model by first outlining the scenario of interest and briefly specifying its sub-modules including mobility, propagation, beamforming, and dynamic blockage models. Finally, we introduce the connectivity process and define the metrics on interest.

Illustrative Scenario. We address a fire suppression mission as a representative example for the evaluation of mmWave mesh network performance in a realistic single-floor indoor deployment, see Fig. 1. Specifically, we consider a team of firefighters operating on the floor of an office building. The team utilizes assisting media applications enabled by the mmWave mesh. These acquire their information streams from the firefighters' on-body video cameras and transmit

them to the command center. The latter processes the video streams and develops an optimized team operation strategy, which provides digital assistance and guidance to the firefighters. In this setup, we assume that the communications infrastructure inside the building is not operational. Connectivity with the command center is provided via a relay node (access point) installed by the rescue team near a window.

Node Mobility Model. To capture the mobility of nodes, we assume that they move around by following the random direction mobility (RDM, [14]) model. Accordingly, a node first randomly chooses its direction of movement uniformly in $(0, 2\pi)$ and then proceeds in this direction at the constant speed v_B for an exponentially distributed time interval with the parameter $\gamma = 1/E[\tau]$, where τ is the mean movement duration. The process is restarted at each stopping point. If during such movement an obstacle is encountered, the node chooses a new direction.

Propagation Model. The received signal power at a mesh node is given by

$$P_R(x) = P_T G_T G_R - PL, \tag{1}$$

where P_T is the transmit power, G_T and G_R are the antenna gains at the transmitter and the receiver sides, respectively, which depend on the antenna array (these parameters can be obtained from the beamforming model introduced in the following subsection), PL is the path loss. Following 3GPP TR 38.901, the mmWave path loss in dB for the line-of-sight (LoS) links is given by

$$PL_{InH-LOS} = 32.4 + 17.3 \lg(d_{3D}) + 20 \lg(f_c), \tag{2}$$

where f_c is the center frequency, d_{3D} is the three-dimensional distance between the radio interfaces of two communicating nodes.

For the non-LoS (NLoS) links, the path loss is determined as

$$PL_{InH-NLOS} = \max(PL_{InH-LOS},\ PL'_{InH-NLOS}), \tag{3}$$

where

$$PL'_{InH-NLOS} = 38.3lg(d_{3D}) + 17.3 + 24.9 \lg(f_c). \tag{4}$$

Beamforming Model. We assume linear antenna arrays at both the transmitter and the receiver sides [15]. Half-power beamwidth (HPBW) of the array, α, is defined as [16]

$$\alpha = 2|\theta_m - \theta_{3db}|, \tag{5}$$

where θ_{3db} is the 3-dB point and $\theta_m = \arccos(-\beta/\pi)$ is the array maximum, while β is the array direction angle. Letting $\beta = 0$, the upper and lower 3-dB points are

$$\theta^{\pm}_{3db} = \arccos[-\beta \pm 2.782/(N\pi)], \tag{6}$$

where N is the number of antenna elements.

Finally, the mean antenna gain over HPBW is expressed as [16]

$$G = \frac{1}{\theta_{3db}^{+} - \theta_{3db}^{-}} \int_{\theta_{3db}^{-}}^{\theta_{3db}^{+}} \frac{\sin(N\pi\cos(\theta)/2)}{\sin(\pi\cos(\theta)/2)} d\theta. \tag{7}$$

Dynamic Blockage Model. In this paper, we consider three types of blockage: (i) blockage by inherent indoor constructions, e.g., walls, furniture; (ii) self-blockage; and (iii) dynamic blockage by environmental objects. The former option is captured by the considered propagation model introduced in the previous subsection. Self-blockage refers to particular positioning of a node, such that it may no longer beamform its antenna towards the intended recipient.

We also follow a dynamic spatially-temporal blockage model. Accordingly, blockers appear at a randomly chosen position that is uniformly distributed over the area of the floor according to a homogeneous temporal Poisson process with the intensity λ. Each blocker is assumed to exist for an exponentially distributed period of time with the mean $1/\mu$. Observe that this stochastic process is inherently of M/M/∞ type, and the number of active blockers is provided by the Poisson distribution with the parameter λ/μ. Given the radius of a blocker, r_B, the fraction of the floor covered by this type of blockers can be obtained by using integral geometry formulations as follows [17]

$$p_C = (1 - f_{C,1})^{\lambda/\mu},\ p_{C,1} = \frac{2\pi S_B}{2\pi(S_A + S_B) + L_A L_B}, \tag{8}$$

where S_A is the floor area and $S_B = \pi r_B^2$ is the blocker radius.

Connectivity and Metrics of Interest. To improve system performance, we assume that a single node supports 3GPP multi-connectivity operation as described in Rel.-15 NR specifications (see TS 37.340) [5]. Accordingly, a node supports multiple connections to its adjacent systems simultaneously, and may dynamically switch between them in case where its current connection is unavailable. In our study, the number of simultaneously supported connections, known as the degree of multi-connectivity, is assumed to be M. It should be noted that depending on the locations of the nodes forming the mesh, the actual number of connections at any given instant of time can be less than M.

In our study, we address connectivity and throughput related performance indicators. These are: (i) the fraction of time when at least one node is disconnected from the mesh network, (ii) the mean number of disconnected nodes at an arbitrary instant of time, and (iii) the mean per-node throughput.

3 Simulation Framework

3.1 Simulator Design

For the numerical evaluation of the mmWave mesh system performance, we develop a custom simulator based on the Stage simulator code [18,19].

The primary part of this tool is a 3D model of an office floor, see Fig. 2. This model allows to assess whether there is a LoS condition between two points in the coordinate plane. The simulation process starts with the coordinate simulation of the node mobility and dynamic blockage. At each iteration, the tool checks the LoS condition between all of the nodes of the mesh. When verifying it, the antenna directivity is also taken into account. The results are stored in the SQL database.

The second phase utilizes the results obtained during the first phase for evaluating the parameters of interests. It starts with the calculation of path losses between all the nodes by using the system model described in Sect. 2. If the signal strength between the two nodes (at the receiver side) is lower than a preset threshold, the simulator assumes that there is no direct connection between these nodes. If there is a connection between them, the tool calculates the throughput by using the Shannon–Hartley theorem for all pairs of nodes in the mesh wherever a direct connection is available. This part abstracts the physical layer of the network. In the next step, the simulator considers radio channels between the nodes, including the medium access control procedures. This delivers a channel topology graph. The third step mimics addressing and routing within the mesh topology as delivered by the second step.

The developed framework is flexible for further extensions. The modifications (e.g., implementation of alternative protocols or applications) can be pursued by applying modified SQL scripts on the coordinate simulation traces stored in the SQL database, without launching a new simulation.

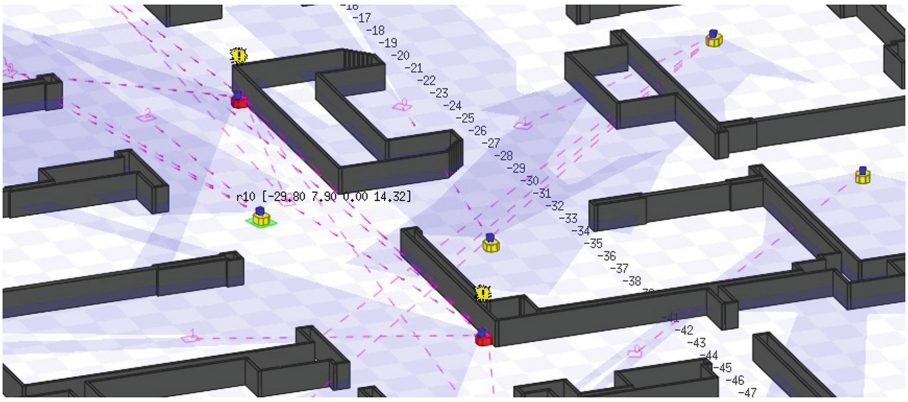

Fig. 2. Three-dimensional view of mesh nodes in simulated layout.

3.2 Data Collection and Analysis

A simulation campaign has been carried out to obtain the metrics of interest by relying on the following procedure. For each considered set of input parameters (termed a round), simulations were set to run for 1200 s of the system time, with

Table 1. Simulation parameters.

Parameter	Value
Operating frequency, f_c	28 GHz
Antenna array	16×16 el. (planar array)
Channel model	3GPP InH
Transmit power	1 W
Receiver sensitivity	-91 dBm
Fraction of floor covered by blockers, p_C	0.15
Number of fire crew members	$\{8, 10, 12, 14, 16\}$
Velocity of crew members	1 m/s
Mobility of crew members	RDM model
Number of simultaneously supported links	$\{2, 3, 4, \infty\}$
Number of iterations per simulation round	4800

a 0.25 change of the system time at each iteration of simulations. The chosen duration of a simulation round approximately corresponds to the time required for checking the floor of the considered size by the rescue team (e.g., firefighters).

Statistical data has only been collected during the steady-state period. The starting point of the steady-state period was detected by utilizing the exponentially-weighted moving average (EWMA) statistics with the weighting parameter set to 0.05 and by employing the procedure from [20].

To remove the residual correlations in the statistical data, we used the batch means strategy. Accordingly, the entire steady-state period duration has been subdivided into 1000 data blocks. The metrics of interest computed for these periods were treated as independent to form statistical samples. The output values for the metrics of interest have been estimated by processing the respective samples.

4 Numerical Results

In this section, we report our numerical results for the mmWave mesh performance in indoor environments. The default system parameters are summarized in Table 1.

Indoor deployments of mmWave systems are characterized by much higher complexity as compared to widely considered outdoor scenarios. Hence, to develop intuition about the system under investigation we start our analysis by assessing the time-dependent behavior of connectivity and throughput processes for three randomly selected mesh nodes as illustrated in Fig. 3. Observing the connectivity performance shown in Fig. 3(a), where 0 indicates the connectivity periods and 1 implies the absence of an active connection, one may conclude that connectivity intervals are rather long as compared to outages. The outage intervals are considerably short but their periodicity is relatively high. This behavior

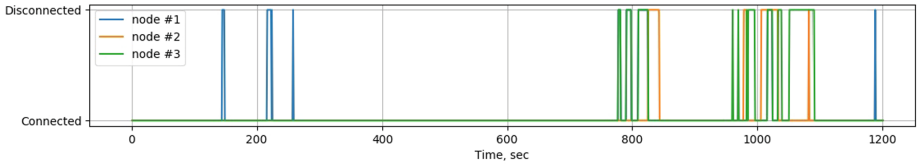

(a) Connectivity trace

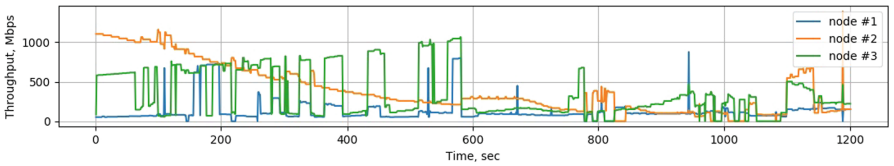

(b) Throughput trace

Fig. 3. Time-dependent behavior of connectivity and throughput.

is a consequence of the realistic indoor deployment and mobility models, where layout features and dynamic blockage result in many short-lived outage events.

The associated throughput of the nodes is illustrated in Fig. 3(b), where the averaging interval was set to 1 s. As one may observe, the throughput may drastically deviate during the connectivity intervals. For some nodes, these fluctuations are rather smooth but one may also notice many sharp peaks in the perceived throughput. Note that the mobility of nodes primarily results in smooth deviations while quick jumps are associated with the blockage process (floor layout geometry and dynamic blockage events).

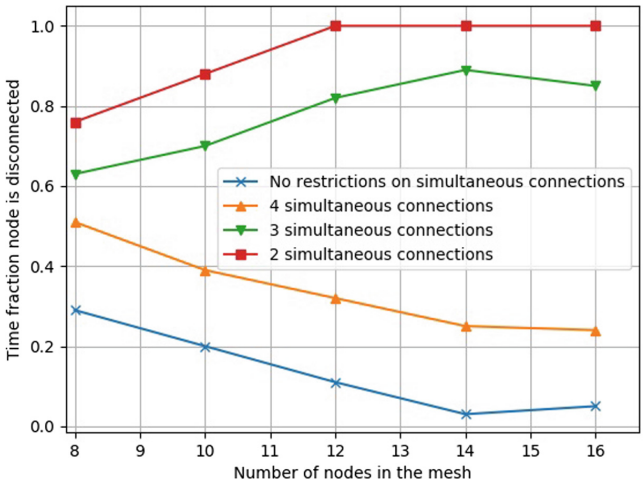

Fig. 4. Time fraction when at least one node is disconnected.

After observing the time-dependent behavior of the system, we proceed by analyzing the stationary state metrics. We start with the time fraction when at least one node is disconnected from the network; it is illustrated in Fig. 4 as a function of the number of nodes in the mesh network and the number of simultaneously supported links, M. Note that this parameter can be considered as an integral measure of the mesh network connectivity, which characterizes the fraction of time when at least one node does not have access to the gateway. One may observe that as the number of nodes increases, and depending on the degree of multi-connectivity, the analyzed value demonstrate fundamentally different behavior.

For $M = 2$ and $M = 3$, the time fraction when at least one node is disconnected increases as the number of nodes in a mesh grows. The rationale behind this behavior is straightforward: for a larger node count the probability that at least one node finds itself in unfavorable position becomes higher, and multi-connectivity may be insufficient to overcome this. However, as the degree of multi-connectivity grows further, the effects of diversity start to dominate when the number of nodes increases. Therefore, we may conclude that multi-connectivity operation in mmWave systems may drastically improve mesh connectivity for indoor deployments. However, the number of simultaneously supported links might be rather high, thus resulting in significant control overheads.

We can now characterize the mesh network connectivity quantitatively in the stationary state. Figure 5 reports the mean number of disconnected nodes as a function of the total number of nodes and the degree of multi-connectivity. Similarly to Fig. 4, we may observe that the degrees of multi-connectivity of $M = 2$ and $M = 3$ do not permit the network to scale appropriately as the mean number of disconnected nodes starts to grow. However, increasing M further to 4 allows this value to remain well below one. One may also notice that if we do not limit the number of simultaneously supported links, the mean number of nodes actually decreases as the number of disconnected nodes in the mesh network grows.

Finally, Fig. 6 studies the mean per-node throughput as a function of the number of nodes in the mesh and the degree of multi-connectivity. As one may notice, this parameter exhibits qualitatively similar behavior for all the values of M. Comparing the mean throughput results corresponding to $M = \infty$ and $M = 2$, one of the key observations here is that the system operates in blockage-limited conditions for the realistic values of M. Indeed, when imposing no restrictions on the degree of multi-connectivity, the per-node throughput is $3 - 4$ times higher as compared to the case of $M = 2$. It is also important to note that for higher degrees of multi-connectivity the system approaches this regime rather slowly, e.g., the mean per-node throughput obtained with $M = 4$ is still approximately half of that for $M = \infty$. This behavior is different from the one reported for outdoor scenarios in, e.g., [7,8], where both capacity and outage probabilities grow exponentially with M.

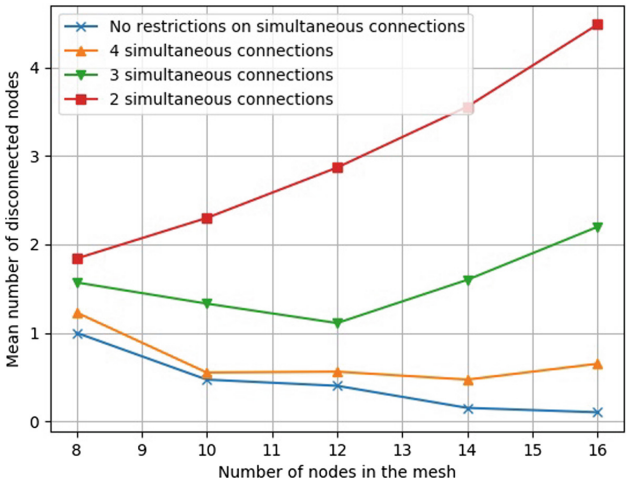

Fig. 5. Mean number of disconnected nodes.

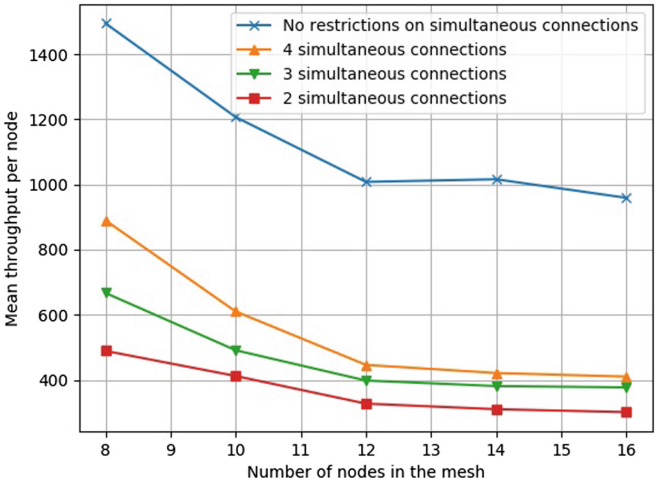

Fig. 6. Mean per-node throughput in mesh network.

5 Conclusion

Motivated by the need for on-demand and high throughput mesh networking in indoor PPDR use cases, we investigated the capabilities of mmWave technology to support these types of applications. Our developed model employed system-level simulations of the mesh system with node mobility, 3GPP-like indoor propagation, dynamical link blockage, and multi-connectivity operation, all for a realistic indoor layout. In this study, the metrics of interest were related to network connectivity and throughput.

Our simulation campaign revealed that the connectivity of individual nodes in indoor environments is characterized by frequent short-lived outage events and causes sharp fluctuations in node throughput even in the presence of multi-connectivity capabilities. Hence, multi-connectivity operation may significantly improve the overall network performance in terms of the fraction of time when at least one node is disconnected as well as the mean number of disconnected nodes. However, the associated increase in per-node performance is less noticeable, which implies that indoor mmWave mesh deployments primarily operate in a blockage-rich environment. This is different from outdoor deployments, where multi-connectivity improves both the connectivity and throughput performance exponentially [7,8].

References

1. Al-samman, A.M., Azmi, M.H., Rahman, T.A.: A survey of millimeter wave (mm-wave) communications for 5G: channel measurement below and above 6 GHz. In: Saeed, F., Gazem, N., Mohammed, F., Busalim, A. (eds.) IRICT 2018. AISC, vol. 843, pp. 451–463. Springer, Cham (2019). https://doi.org/10.1007/978-3-319-99007-1_43
2. Singh, S., Mudumbai, R., Madhow, U.: Interference analysis for highly directional 60-GHz mesh networks: the case for rethinking medium access control. IEEE/ACM Trans. Netw. (TON) **19**(5), 1513–1527 (2011)
3. Cheffena, M.: Industrial wireless communications over the millimeter wave spectrum: opportunities and challenges. IEEE Commun. Mag. **54**(9), 66–72 (2016)
4. Humpleman, R., Watson, P.: Investigation of attenuation by rainfall at 60 GHz. In: Proceedings of the Institution of Electrical Engineers, vol. 125, pp. 85–91. IET (1978)
5. 3GPP: NR; Multi-connectivity; Overall description (Release 15), 3GPP TS 37.340 V15.2.0, June 2018
6. Moltchanov, D., Ometov, A., Andreev, S., Koucheryavy, Y.: Upper bound on capacity of 5G mmWave cellular with multi-connectivity capabilities. Electron. Lett. **54**(11), 724–726 (2018)
7. Gapeyenko, M., et al.: On the degree of multi-connectivity in 5G millimeter-wave cellular urban deployments. IEEE Trans. Veh. Technol. **68**(2), 1973–1978 (2019)
8. Gerasimenko, M., Moltchanov, D., Gapeyenko, M., Andreev, S., Koucheryavy, Y.: Capacity of multi-connectivity mmWave systems with dynamic blockage and directional antennas. IEEE Trans. Veh. Technol. **68**(4), 3534–3549 (2019)
9. Petrov, V., et al.: Dynamic multi-connectivity performance in ultra-dense urban mmWave deployments. IEEE J. Sel. Areas Commun. **35**(9), 2038–2055 (2017)
10. Polese, M., Giordani, M., Mezzavilla, M., Rangan, S., Zorzi, M.: Improved handover through dual connectivity in 5G mmWave mobile networks. IEEE J. Sel. Areas Commun. **35**(9), 2069–2084 (2017)
11. Niu, Y., Li, Y., Jin, D., Su, L., Vasilakos, A.V.: A survey of millimeter wave communications (mmWave) for 5G: opportunities and challenges. Wirel. Netw. **21**(8), 2657–2676 (2015)
12. Thornburg, A., Bai, T., Heath Jr., R.W.: Performance analysis of outdoor mmWave ad hoc networks. IEEE Trans. Signal Process. **64**(15), 4065–4079 (2016)

13. Qiao, J., Shen, X.S., Mark, J.W., Shen, Q., He, Y., Lei, L.: Enabling device-to-device communications in millimeter-wave 5G cellular networks. IEEE Commun. Mag. **53**(1), 209–215 (2015)
14. Nain, P., Towsley, D., Liu, B., Liu, Z.: Properties of random direction models. In: Proceedings of 24th Annual Joint Conference of the IEEE Computer and Communications Societies, vol. 3, pp. 1897–1907. IEEE (2005)
15. Petrov, V., Komarov, M., Moltchanov, D., Jornet, J.M., Koucheryavy, Y.: Interference and SINR in millimeter wave and terahertz communication systems with blocking and directional antennas. IEEE Trans. Wirel. Commun. **16**(3), 1791–1808 (2017)
16. Balanis, C.A.: Antenna Theory: Analysis and Design. Wiley, Hoboken (2016)
17. Petrov, V., Moltchanov, D., Kustarev, P., Jornet, J.M., Koucheryavy, Y.: On the use of integral geometry for interference modeling and analysis in wireless networks. IEEE Commun. Lett. **20**(12), 2530–2533 (2016)
18. Vaughan, R.: Massively multi-robot simulation in stage. Swarm Intell. **2**(2–4), 189–208 (2008)
19. Gerkey, B., Vaughan, R.T., Howard, A.: The player/stage project: tools for multi-robot and distributed sensor systems. In: Proceedings of the 11th International Conference on Advanced Robotics, vol. 1, pp. 317–323 (2003)
20. Perros, H.: Computer simulation techniques. The definitive introduction. North Carolina State University (2009)